

EXERGY LOSS ANALYSIS OF THE REGENERATOR IN A SOLAR STIRLING ENGINE

by

Wenlian YE^{a, b}, Zhe YANG^a, and Yingwen LIU^{a*}

^a Key Laboratory of Thermo-Fluid Science and Engineering of MOE, School of Energy and Power Engineering, Xi'an Jiaotong University, Xi'an, China

^b Key Laboratory of Vacuum Technology and Physics, Lanzhou Institute of Physics, Lanzhou, Gansu, China

Original scientific paper

<https://doi.org/10.2298/TSCI170911058Y>

In order to evaluate the irreversibility and exergy losses of the regenerators in a solar beta-type free piston Stirling engine due to flow friction, 1-D thermodynamic model to quantify exergy loss in the regenerators are built. The effects of important parameters, such as oscillating flow pressure drop, the exergy loss to flow friction, the exergy losses to conduction heat transfer at the hot and cold side of the regenerator and the percentage of Carnot efficiency of Stirling engine are presented and studied in detail. Results show that exergy loss decreases with the increase of the porosity and matrix diameter. As for the regenerator length, there is an optimum value that is equal to 0.035 m where the exergy loss is minimal and the percentage of Carnot efficiency is maximal. Therefore, some parameters should be selected reasonably to meet the overall design requirements of a solar Stirling engine.

Key words: regenerator, exergy loss, Carnot efficiency, Stirling engine

Introduction

In recent years, solar energy has been concerned increasingly with the serious energy problem. Dish-Stirling solar power generation system is one of the solar energy utilities and has a broad prospect. Dish-Stirling systems have demonstrated good efficiency of any solar power generation system [1]. Stirling engines operate in a closed cycle with a working fluid of Helium. Working fluid is circulated in two working spaces (compression space and expansion space) and three heat exchangers (a cooler, a regenerator and a heater) [2]. A solar free piston Stirling engine (FPSE) is presented in this paper. A regenerator, as a key component in a Stirling engine, plays an extremely important role in improving the efficiency of the Stirling engine, and it always works in oscillating flow. The exergy loss of the regenerator directly determines the efficiency of the whole system. Moreover, the efficiency of Stirling engine mainly depends on the exergy loss of the regenerator which is influenced by the porosity, heat transfer coefficient, mass flow and the dead volume of regenerator [3].

Some researchers have proposed a variety of methods for characterizing the heat transfer of the regenerator under the condition of oscillating flow. Qvale and Smith [4] as-

* Corresponding author, e-mail: ywliu@xjtu.edu.cn

sumed sinusoidal pressure variation and mass flow rate with a phase angle between them, and obtained an approximate solution for the thermal performance of a Stirling engine regenerator. Ercan [5] carried out the numerical study of the regenerators of free-piston Stirling engines using Lagrangian formulation.

Many methods were used for simulating the oscillatory flow of the regenerator like CFD, Sage, and DeltaEC [6, 7], *etc.* For modeling the physical mechanism of the actual Stirling engine, Sage [8, 9] was employed to quantify its irreversibility, and it has been used by NASA GRC to predict and improve the performance of Stirling engine for a long time [10-12]. As a powerful method for the design and analysis of thermal systems, exergy loss analysis has been used to quantify exergy loss flow and exergy destruction in pulse tube cryocooler [13].

In this paper, a Sage model for a solar beta-type FPSE is developed to analyze and optimize its performance. Exergy losses due to flow friction and conduction heat transfer of fluid, matrix and the regenerator wall between the hot end and cold end of the regenerator are identified. Meanwhile, the percentage of Carnot efficiency of Stirling engine has been investigated.

Model description

Figure 1 presents the schematic diagram of a solar Stirling generator. This structure is a beta-type free piston Stirling generator (FPSG). It consists of a Stirling engine and a linear generator. The engine includes a heater, a regenerator, a cooler, as well as a piston and a displacer situated at 60° angles to each other. The power piston and displacer are supported by flexures. Helium with mean pressure of 3.5 MPa is used as the working gas. The initial hot and cold end temperature of the regenerator is 923 K and 323 K, respectively.

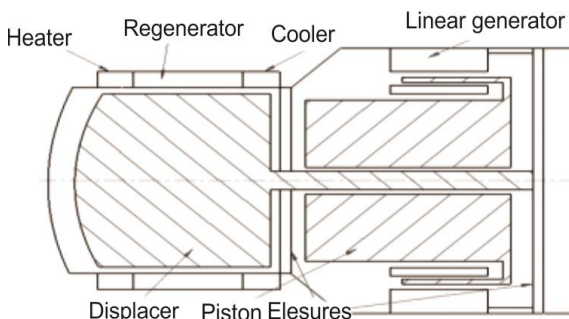


Figure 1. Schematic diagram of beta-type FPSE

In the regenerator model with a woven screen matrix of the FPSE, there are several exergy losses that must be taken into account. These are: (1) exergy loss to heat conduction directly through the cylinder wall, (2) exergy loss to heat conduction through the steel matrix, (3) exergy loss to heat conduction through the working gas in the regenerator, and (4) the exergy loss to flow friction. This model assumed a conduction boundary condition between the woven screen matrix and the cylinder wall. Input parameters to Sage-based model of the regenerator include regenerator length, porosity, wire diameter, *etc.* The output results are exergy loss to flow friction and heat flow, *etc.*

Exergy loss analysis

The method of exergy analysis is based on the Second law of thermodynamics and the concept of irreversible production of entropy. Similar to most Stirling engines, the major loss occurs within the regenerator. Figure 2 depicts important parameters used in quantifying the interaction of pressure with regenerator. The parameters M and p are the amplitudes of mass flow and pressure, respectively.

There are three exergy losses to conduction heat transfer between the hot end and cold end because of huge temperature gradient. The entropy generation of heat flow can be expressed:

$$S_{\text{cond}} = -\oint \oint \frac{q\Delta T}{T^2} \quad (1)$$

where q is the normal heat flow (conduction heat transfer) and ΔT represents the temperature difference. Entropy generations are expressed as exergy outputs by multiplying the entropy integrals by T_o , the normalization temperature of the root Stirling model component:

$$E_{\text{cond}} = -T_o \oint \oint \frac{q\Delta T}{T^2} \quad (2)$$

The porous metals used in the regenerator could also cause the flow resistance loss due to the generation of inevitable pressure drop. The entropy generation of viscous friction, in 1-D flow, may be calculated:

$$S_{\text{flow}} = -\oint \oint \frac{uA\nabla P}{T} \quad (3)$$

where uA is the volumetric flow rate and ∇P represents that part of the pressure gradient due to viscous friction. Then the exergy output is defined:

$$E_{\text{flow}} = -T_o \oint \oint \frac{uA\nabla P}{T} \quad (4)$$

According to the previous equations, the exergy balance for the regenerator system is defined:

$$E_{\text{loss}} = E_{\text{in}} - E_{\text{out}} = E_{\text{cond}} + E_{\text{flow}} \quad (5)$$

where E_{in} and E_{out} are the inlet and outlet exergy, respectively, and E_{loss} is the total exergy loss of the regenerator.

In order to evaluate the performance of the Stirling engine, we define the percentage of Carnot efficiency:

$$\eta_{\text{eff}} = \frac{W_{\text{net}}}{Q_{\text{in}}} \quad (6)$$

$$\eta = \frac{\eta_{\text{eff}}}{\eta_{\text{Carnot}}} \quad (7)$$

where Q_{in} is the absorbed heat by the heater, W_{net} – the net power of compressing consumption, and expanding work, η_{eff} – the actual thermal efficiency, and η_{Carnot} is the Carnot cycle efficiency.

Results and discussion

Figure 3 shows that the pressure drop varies with different lengths of regenerator when the regenerator diameter is fixed in the whole model. For the operating frequency of 50 Hz, the amplitude value of pressure drop in oscillating flow increases from 0.036 MPa to 0.098 MPa when the length increases from 0.025 m to 0.07 m. The reason is that the flow friction in



Figure 2. Regenerator schematic with important modeling parameters

the regenerator is proportional to its length, resulting in the increase of the flow friction while the axial pressure drop increases. In short, the change of axial pressure drop will affect the exergy loss to flow friction.

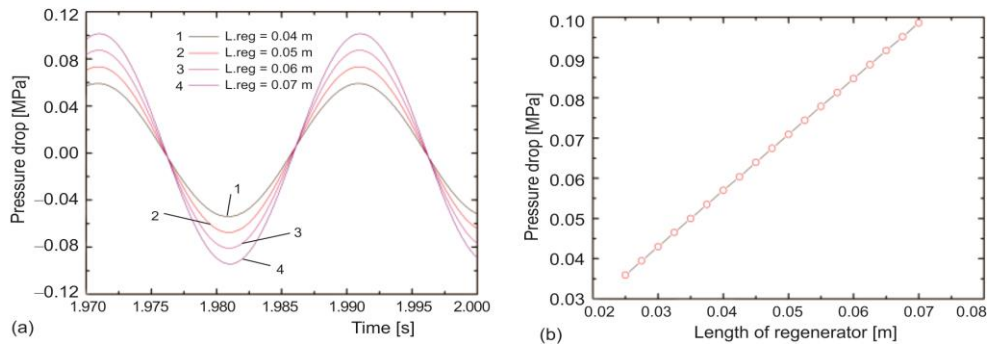


Figure 3. Pressure drop variation with length for (a) oscillating flow and (b) amplitude value

Figure 4 shows the total exergy loss, E_{loss} , and exergy loss distribution of heat conduction and flow friction of the regenerator at different regenerator lengths. In fig. 4(a), the exergy loss to flow friction, E_{flow} , increases with the increase of the regenerator's length. The pressure drop in the regenerator is mainly affected by its length. If neglecting the change of physical property and keeping other parameters unchangeable, the pressure drop and exergy loss in the regenerator varies almost linearly with its length. The exergy losses to heat conduction of matrix and fluid, E_{matrix} and E_{fluid} , is also related to the length, and the temperature difference between the inlet (hot-end) and outlet (cold-end) decreases with the increase of its length. The exergy loss to heat conduction of wall, E_{wall} , decreases much more rapidly than E_{fluid} and E_{matrix} , the reason is that the temperature difference, ΔT , of hot end and cold end of wall is not changed so much, while the ΔT of fluid and matrix increases. Therefore, the total exergy loss decreases when the length changes from 0.025 m to 0.035 m, and then increases.

In fig. 4(b), the description of E_{cond} accounts for the largest proportion of 72% to 21% as evidenced by a large regenerator length and a short temperature difference. However, the description of E_{flow} accounts for 28% to 79%, which can surely be reduced by improving the design of the regenerator. This result above indicates that E_{flow} and E_{cond} are sensitive to regenerator length.

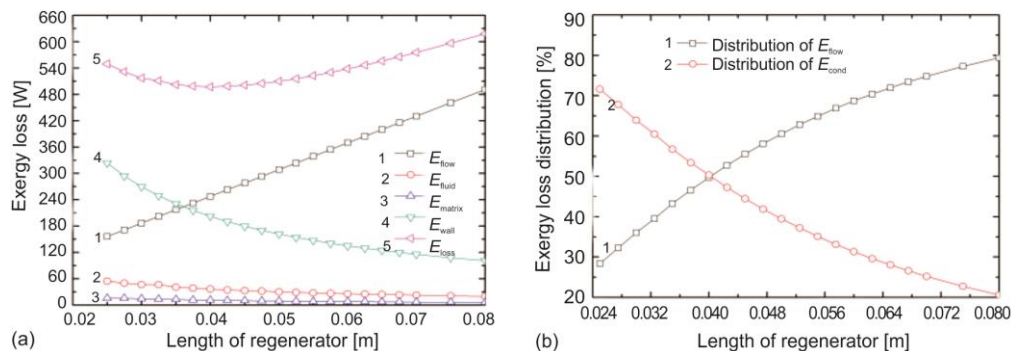


Figure 4. Exergy loss variation with length for (a) exergy losses and (b) exergy loss distribution

Figure 5 shows the total exergy loss, E_{loss} , and the percentage of Carnot efficiency, η , of Stirling engine at different regenerator lengths. The E_{loss} increases with the decrease of regenerator length from 0.025 m to 0.04 m and then increases rapidly. The η firstly increases. When the length reaches approximately 0.035 m, it reaches its maximum value and then decreases rapidly with the increase of regenerator length. These results indicate that the length of regenerator is an important parameter that should be optimized in the design to obtain a preferred thermal efficiency. Furthermore, for the regenerator with a specific diameter, there should be an optimal length of the regenerator where the minimal total E_{loss} can be achieved.

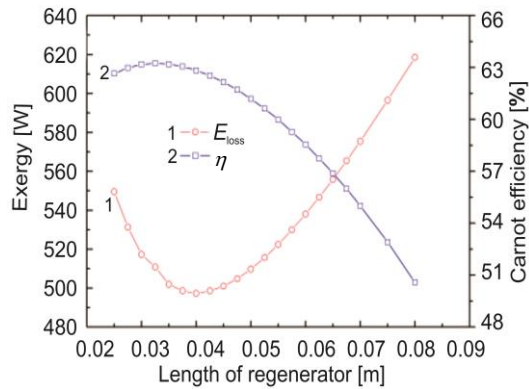


Figure 5. Exergy loss and percentage of Carnot efficiency variation with length

In the model, the matrix diameter and the length of regenerator are fixed. The mass flow under oscillating flow is nearly not changed. Figure 6 shows the pressure drop under oscillating flow and the amplitude value of pressure drop with porosity ranging from 0.7 to 0.85. From fig. 6, it can be seen that when increasing porosity, pressure drop will decrease from 0.17 MPa to 0.038 MPa. The reason is that the large porosity leads to the increase of the free flow area and low friction factor. Therefore, flow friction loss will also decrease. However, the performance of heat transfer will be worse because of the decrease of the heat transfer area. In sum, porosity becomes increasingly sensitive to pressure drop. These results above suggest that the suitable porosity should be considered to improve the performance of the regenerator.

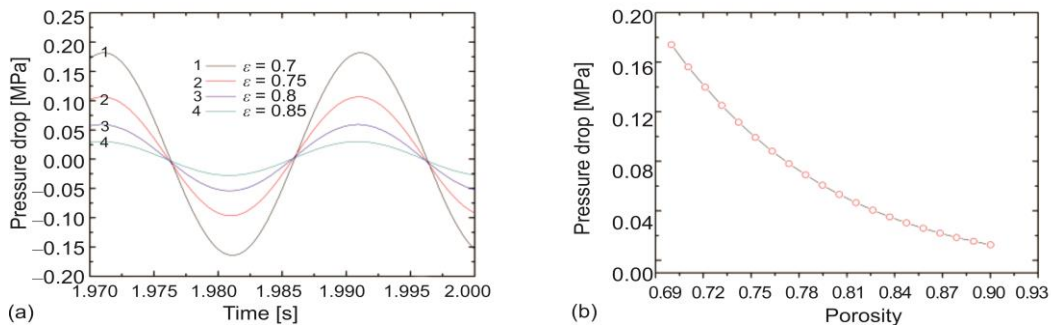


Figure 6. Pressure drop variation with porosity for (a) oscillating flow and (b) amplitude value

Figure 7 shows the exergy losses, E_{loss} , E_{flow} , E_{matrix} , E_{fluid} , E_{wall} , and exergy loss distribution, E_{flow} , E_{cond} , at different porosity. In fig. 7(a), E_{flow} and E_{loss} in the regenerator decrease with the increase in porosity. The reason is that the pressure drop in the regenerator decreases with the reducing of the flow velocity because of big porosity. The exergy losses to heat conduction of the wall, the fluid and the matrix change slightly. For instance, E_{flow} and E_{loss} decrease from 734 W to 55 W and from 998 W to 308 W, respectively. In fig. 7(b), the distribution of E_{flow} accounts for 75 % to 15 % because of a large pressure drop. The distribution of exergy loss to heat conduction, E_{cond} , increases from 25% to 85%. This result indi-

icates that E_{flow} is much more sensitive to the porosity of the regenerator. The capacity of heat storage decreases with the porosity increasing. In other words, when the number of filled screen decreases or the porosity decreases, the heat transfer area per unit volume will decrease quickly. At the same time, the flow area increases, and the pressure drop decreases, then E_{flow} decreases. Therefore, several requirements on the regenerator are contradictory, focusing on the requirements of the porosity. The pressure drop should be reduced by increasing porosity while the porosity should be reduced to achieve a good thermal performance. Consequently, porosity should be chosen rationally during the practical work in subsequent.

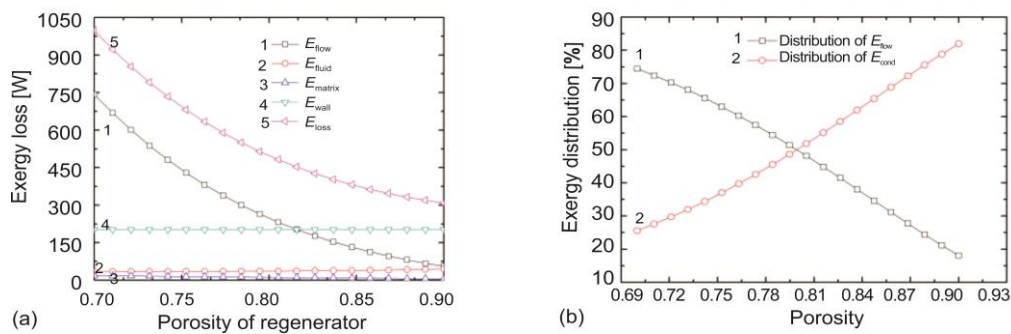


Figure 7. Exergy loss variation with porosity for (a) exergy losses and (b) exergy loss distribution

Figure 8 plots the total exergy loss, E_{loss} , and the percentage of Carnot efficiency, η , of Stirling engine at different regenerator porosity. It can be showed that a higher porosity will result in higher η and lower E_{loss} . The E_{loss} changes linearly with the porosity varying from 0.7 to 0.85, and then decreases slowly (from 0.85 to 0.9). Results show that the Stirling engine will achieve a maximum η at a porosity of 0.85 to 0.88.

According to the previous results, the optimum design between E_{flow} and E_{cond} is determined by both the porosity and the matrix diameter. The change of matrix diameter affects the porosity simultaneously. For a given regenerator length of 0.4 m, the relationship between the matrix diameter and pressure drop of the regenerator is studied in this section.

Figure 9 reveals the pressure drop at different matrix diameters from $1.5 \cdot 10^{-5}$ m to $3.0 \cdot 10^{-5}$ m. As can be seen in fig. 9, increasing matrix diameter results in the decrease of pressure drop. For instance, the amplitude value of pressure drop is 0.14 MPa for the d_m of $1.5 \cdot 10^{-5}$ m, and the 0.41 MPa for the $3.0 \cdot 10^{-5}$ m, respectively, as shown in fig. 9(b). It should be noted that the decrease of matrix diameter leads to the change of the resistance structure. Therefore, the heat transfer area of the matrix becomes larger, resulting in a better characteristic of heat conduction and less pressure drop. It is helpful to increase the performance of the Stirling engine.

Figure 10 shows the diagram of the exergy losses vs. matrix diameter. The exergy loss to flow friction, E_{flow} , and total exergy loss, E_{loss} , decreases gradually with the increase of matrix diameter, and other exergy losses to heat conduction increase slowly in fig. 10(a). As a

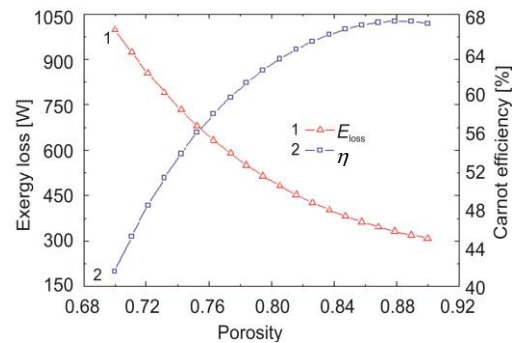


Figure 8. Exergy loss and percentage of Carnot efficiency variation with porosity

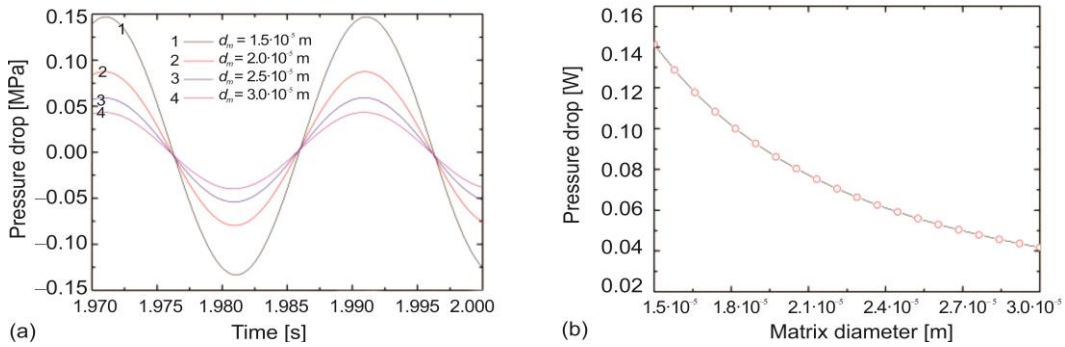


Figure 9. Pressure drop variation with matrix diameter for (a) oscillating flow and (b) amplitude value

matter of fact, E_{cond} is proportional to the cross-sectional area, the temperature difference at inlet and outlet, and the regenerator length while the change of temperature difference is nearly small. Consequently, E_{fluid} loss increases from 27 W to 40 W.

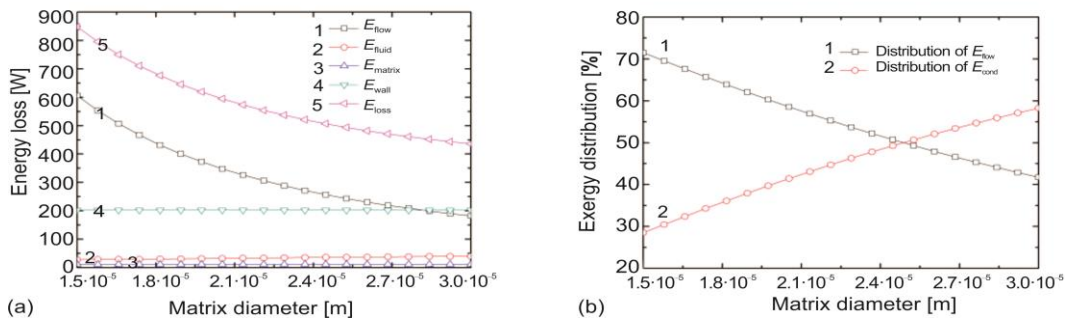


Figure 10. Exergy loss variation with matrix diameter for (a) exergy losses and (b) exergy loss distribution

In addition, the decrease of pressure drop (shown in fig. 9) leads to the reduction of E_{flow} . Hence, the E_{loss} decreases. In fig. 10(b), the distribution of E_{flow} accounts for 72% to 42% and the E_{cond} ratio changes from 28% to 58%. These previous results indicate that the increase of the matrix diameter can reduce the pressure drop. The pressure drop

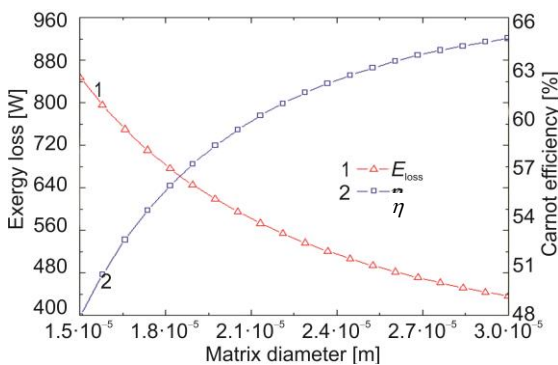


Figure 11. Exergy loss and percentage of Carnot efficiency variation with matrix diameter

loss decreases rapidly, which can effectively reduce the E_{flow} of the regenerator. However, it should be noted that designing a regenerator with such a big matrix diameter might bring some problems in practice.

Figure 11 shows that E_{loss} and η vary with the matrix diameter. As shown in fig. 11, the matrix diameter ranges from $1.5 \cdot 10^{-5}$ to $3.0 \cdot 10^{-5}$ m, at which E_{loss} varies from 850 W to 435 W, and η of Stirling engine varies from 48% to 65% when the length is 0.04 m.

Conclusions

This study is used to quantify losses in an annular regenerator of Stirling engine by changing the length, the porosity and matrix diameter using exergy loss analysis. Results showed that the three parameters of the regenerator of a solar Stirling engine had a significant impact on the total exergy loss statistically. The total exergy loss first increased and then decreased as the length of the regenerator increased. It decreased with an increase of both the porosity and matrix diameter of the regenerator. According to the optimal design and actual operation of the Stirling engine, it reveals that suitable performance can be achieved when the optimal value of the regenerator is with porosity of 0.85, the length of about 0.04 m. However, the results above are preliminary design parameters, and the regenerator is affected by multi-parameters, and its performance needs to be measured in the later experiment. Furthermore, this paper proposes the optimizing design guidelines of the Stirling engine and regenerator to promote its utilization in solar energy.

Acknowledgment

This work is financially supported by the National Natural Science Foundation of China (No. 51576150) and National Key R&D Program of China (2016YFE0204200).

Nomenclature

A	– cross-sectional area, [m ²]	T	– temperature, [K]
L	– length of regenerator, [m]	U	– velocity, [ms ⁻¹]
M	– amplitudes of mass-flow rate, [kgs ⁻¹]	W	– net power, [W]
m	– mass flow rate, [kgs ⁻¹]	<i>Greek symbols</i>	
P	– pressure amplitude, [Pa]	η	– efficiency, [-]
q	– heat flow, [Wm ⁻²]	ω	– angular frequency, [rads ⁻¹]
Q	– heat, [W]		

References

- [1] Theocharis, T., *et al.*, Technical and Economical Evaluation of Solar Thermal Power Generation, *Renewable Energy*, 28 (2003), 6, pp. 873-886
- [2] Slavin, V. S., *et al.*, Conversion of Thermal Energy into Electricity via a Water Pump Operating in Stirling Engine Cycle, *Applied Energy*, 86 (2009), 7, pp. 1162-1169
- [3] Timoumi, Y., *et al.*, Performance Optimization of Stirling Engines, *Renewable Energy*, 33 (2008), 9, pp. 2134-2144
- [4] Ovale, E. B., *et al.*, The Influence of Pressure Cycling on Thermal Regenerators, *ASME Journal of Engineering For Industry*, 89 (1967), 3, pp. 563-569
- [5] Ataer, O. E., Numerical Analysis of Regenerators of Free-Piston Type Stirling Engines Using Lagrangian Formulation, *International Journal of Refrigeration*, 25 (2002), 5, pp. 640-652
- [6] Yang, P., *et al.*, Prediction and Parametric Analysis of Acoustic Streaming in a Thermoacoustic Stirling Heat Engine with a Jet Pump Using Response Surface Methodology, *Applied Thermal Engineering*, 103 (2016), June, pp. 1004-1013
- [7] Yang, P., *et al.*, Application of Response Surface Methodology and Desirability Approach to Investigate and Optimize the Jet Pump in a Thermoacoustic Stirling Heat Engine, *Applied Thermal Engineering*, 127 (2017), Dec., pp. 1005-1014
- [8] Gedeon, D., Sage-Object-Oriented Software for Stirling Machine Design, AIAA, Athens, O., USA, 1994, pp. 94-100
- [9] Gedeon D., *Sage User's Guide*, 9th ed., Gedeon Associates, Athens, O., USA, 2013
- [10] Jonathan, F., *et al.*, Development and Validation of Linear Alternator Models for the Advanced Stirling Converter, NASA/TM-2015-218456, 2015, Washington DC, pp. 1-24
- [11] Ebiana, A. B., *et al.*, An Off-Design Sage Thermodynamic Model of a Scaled Stirling Engine, *Proceedings*, 1st International Energy Conversion Engineering Conference, Ports Mouth, Va., USA, 2003

- [12] Maxwell, H, Implementation of a Sage-Based Stirling Model into a System-Level Numerical Model of the Fission Power System Technology Demonstration Unit, *NASA/TM-2011-217203*, 64 (2011), 6, pp. 200-203
- [13] Razani, A., *et al.*, Exergy Flow in Pulse Tube Refrigerators and their Performance Evaluation Based on Exergy Analysis, *Advances in Cryogenic Engineering*, 710 (2004), 1, pp. 1508-1518